ELSEVIER

Engineering Analysis with Boundary Elements 31 (2007) 402–409

ENGINEERING ANALYSIS with BOUNDARY ELEMENTS

www.elsevier.com/locate/enganabound

Adsorption of His-tagged peptide to Ni, Cu and Au (1 0 0) surfaces: Molecular dynamics simulation

Zhenyu Yang, Ya-Pu Zhao*

State Key Laboratory of Nonlinear Mechanics (LNM), Institute of Mechanics, Chinese Academy of Sciences, Beijing 100080, China

Received 26 February 2006; accepted 5 July 2006
Available online 16 February 2007

Abstract

Molecular dynamics (MD) simulations are performed to study the interaction of His-tagged peptide with three different metal surfaces in explicit water. The equilibrium properties are analyzed by using pair correlation functions (PCF) to give an insight into the behavior of the peptide adsorption to metal surfaces in water solvent. The intermolecular interactions between peptide residues and the metal surfaces are evaluated. By pulling the peptide away from the peptide in the presence of solvent water, peeling forces are obtained and reveal the binding strength of peptide adsorption on nickel, copper and gold. From the analysis of the dynamics properties of the peptide interaction with the metal surfaces, it is shown that the affinity of peptide to Ni surface is the strongest, while on Cu and Au the affinity is a little weaker. In MD simulations including metals, the His-tagged region interacts with the substrate to an extent greater than the other regions. The work presented here reveals various interactions between His-tagged peptide and Ni/Cu/Au surfaces. The interesting affinities and dynamical properties of the peptide are also derived. The results give predictions for the structure of His-tagged peptide adsorbing on three different metal surfaces and show the different affinities between them, which assist the understanding of how peptides behave on metal surfaces and of how designers select amino sequences in molecule devices design.

Keywords: Molecular dynamics; Adsorption; His-tagged peptide; Pair correlation function; Root mean square displacement/deviation; Nanotechnology

1. Introduction

The adsorption of complex molecules on surfaces have recently become the subject of intensive investigation because of the molecules intrinsic properties and prospective applications (e.g. in molecular electronics). The behavior of molecular adsorption on surfaces plays a vital role in the field of nanotechnology, especially in the areas such as nanodevices [1] and molecular recognition [2]. Many specific protein-surface interactions have been observed in natural systems [3] or created using new nano-engineering techniques [4]. There is the possibility of emulating biology in the fabrication of materials, assembling them from the bottom-up with a hierarchy of levels of organization [5]. In the field of nanotechnology, protein-surface interactions constitute the basis for the assembly of interfacial protein, such as sensors, activators and other functional components at biological/electronic junction, etc. [4]. Understanding how polymer molecules behave near metal surfaces would greatly enhance our ability to control the essential interfacial properties in a wide variety of problem, including adhesion, wetting and nano-wetting, biomolecular recognition and self-assembly.

Because of the interaction between protein and metal surfaces is of considerable technological and fundamental interests, much effort has been dived into the development of protein adsorption experiments and simulations. In general, molecular ordering on a surface is controlled by a delicate balance between intermolecular forces and molecule–substrate interactions. Under suitable conditions, these interactions can be tuned by the appropriate choice of substrate material and symmetry. Several studies [1–3,5] have indicated that, upon molecular adsorption, surfaces do not always behave as static templates, but may rearrange dramatically to accommodate different molecular

*Corresponding author. Tel.: +86 10 62658008; fax: +86 10 62561284.
E-mail address: yzhao@lnm.imech.ac.cn (Y.-P. Zhao).

0955-7997/$ - see front matter © 2007 Elsevier Ltd. All rights reserved.
doi:10.1016/j.enganabound.2006.07.012

species. By means of high-resolution, fast-scanning tunneling microscopy (STM) [10], unprecedented new insight has been recently achieved into a number of fundamental processes related to the interaction of largish molecules with surfaces such as molecular diffusion, bonding of adsorbates on surfaces and molecular self-assembly. In addition to the normal imaging mode, the STM tip can also be employed to manipulate single atoms and molecules in a bottom–up fashion, collectively or one by one at a time. In this way, molecule-induced surface restructuring processes can be revealed directly and nanostructures can be engineered with atomic precision to study surface phenomena of fundamental interest.

Recent studies and descriptions about protein-surface interactions intensively focused on developing systems to operate at the nanoscale with the advantage of the functional properties of these novel proteins [4]. Sarikaya et al. [3] have proved polypeptide sequences exhibiting affinity to binding to various solid surfaces including Au, Pt, Pd and so on. His-tagged peptide was used by Montemagno et al. [6] to attach a biomolecular motor, F1-ATPase, to metal substrates, and they have tested the binding strength of a 6×His-tagged synthetic peptide attached to Ni-, Cu- and Au-coated coverslips. Many researchers also have used a variety of informative techniques [7,8] to perform kinetic measurements of adsorbed protein as a function of time and equilibrium adsorption isotherms. Wertz et al. [9] used total internal reflectance fluorescence (TIRF) to infer the orientation and spreading behavior of fibrinogen and lysozyme on hydrophobic and hydrophilic surfaces from kinetic measurements. Schunack et al. [10] observed three different conformations of the molecule on the flat surface terraces at low temperature by STM.

Most simulations of the organic molecules–metal surfaces interactions are from the ab initio calculation and density functional theory (DFT) [11–14], which developed the potentials for the molecules between metals, but they are limited in a rather small scale. By MD methods, Braun et al. [15] simulated multi-peptides interacting with gold of 5 ns. Similarly, Kantarci et al. [16] carried out explicit solvent MD simulations on four different peptide sequences in the absence and presence of the metal surface and analyzed the relationship between sequence, structure and binding process for metal binding peptides.

To gain a better insight into the mechanism of peptide recognition and binding, we carried out MD simulation on His-tagged peptide adsorption on transitional metals: nickel, copper and gold. Explicit solvent simulations are carried out in the absence and presence of the metal surface (1 0 0). We analyze the static properties and dynamics properties. The interactions between His-tagged peptide and water molecules, metal surfaces are discussed. As an analysis of their interactions is presented, this paper provides perception for the common characteristics in static, dynamics properties of these sequences and an analysis of their interactions.

2. Molecular dynamics implementation

The His-tagged peptide investigated here consists of fourteen amino acid residues including six Glycines (Gly), two Lysines (Lys) and six Histidines (His) tagged at the end (Fig. 1). The His-tagged peptide investigated in the present work has the following sequences: Gly-Gly-Lys-Gly-Gly-Lys-Gly-Gly-His-His-His-His-His-His [4]. This His-tagged peptide was tested on three different nanofabricated metal surfaces (Ni, Cu, Au) for the binding strength. Qualitative analysis shows that the affinity of the His-tagged peptide is the strongest for the nickel-coated coverslips followed by the unoxidized copper and gold substrates.

The transferable intermolecular potential 3-point (TIP3P) model [17] is used to describe water–water and solute–water interactions. TIP3P uses atom-centered point charges to represent the electrostatic interactions. The 'bond increment' method for assigning charges is implemented for this force field. Kohlmeyer et al. [18] show that the effect of electronic polarizability has little influence on the structure of water near a metal surface, so the influence can thus be neglected. The Ni, Cu, Au (1 0 0) surfaces composed of three layers are created manually based on their known FCC crystal structures and the lattice parameters are 3.543, 3.615 and 4.070 Å, respectively. The entire metal surfaces, composed of three layers, are about 5 Å thick and approximately 30 Å × 30 Å wide. The metal atoms are fixed to speed up the computations.

For the peptide, the standard amino acid residue topology and parameters [19] based on CHARMM all-atom parameters [20] are used. The non-bonded interactions are based on Lennard-Jones (L-J) 6–12 potential:

$$E(r_{ij}) = 4\varepsilon\left[\left(\frac{\sigma}{r_{ij}}\right)^{12} - \left(\frac{\sigma}{r_{ij}}\right)^{6}\right], \tag{1}$$

where ε is the well depth, σ for the collision diameter, and r_{ij} for the particle distance.

The L-J parameters of three metal atoms are given in Table 1 [21]. Geometry average is taken by combination rules which set L-J interaction parameters between metal atoms and amino acid atoms. MD simulations are

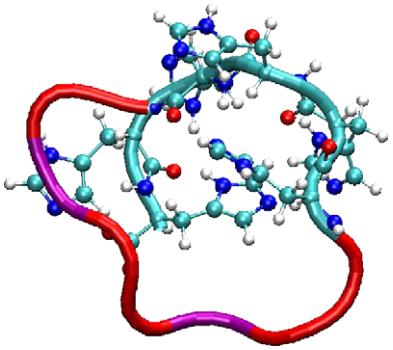

Fig. 1. The His-tagged peptide with sequences: Gly-Gly-Lys-Gly-Gly-Lys-Gly-Gly-His-His-His-His-His-His. The His-tags are also showed in CPK mode.

Table 1
The Lennard-Jones parameters for the metals

Metals	ε/k_B (deg.)	σ (Å)
Nickel	6030	2.282
Copper	4750	2.338
Gold	5123	2.637

performed using the CHARMM28b1 MD simulation package [19]. All simulations are performed at constant volume and temperature ($T = 298$ K) using a Berendsen weak-coupling thermostat [22], with temperature coupling constant 0.2 ps. For solute–water and water–water non-bonded interactions, a twin-range cutoff scheme with 10 and 14 Å cutoff radii was applied. The non-bonded interactions in the range between theses radii are updated every fifth time step, together with the pair list update. A time step of 1 fs is used and bond lengths were constrained by the SHAKE algorithm [23]. Each system is simulated with periodic boundary conditions (PBC).

For all the simulations, the peptide is equilibrated in water for a 1.2 ns MD run and then manually placed next to the metal surfaces. For the periodic box containing surface, peptide, and water molecules, independent MD simulations were performed after a brief energy minimization to resolve undesirable close contacts among the different components in the system. The resulting orthogonal box dimensions including the surface, peptide, and water molecules are 30 Å × 30 Å × 30 Å (Fig. 2(a)). The number of residues in the His-tagged peptide is 192 and the total number of atoms including water and metal surface varies between 2338 and 2404.

With similar procedures, additional dynamic simulations to pull the peptide away from the metal substrates after 2 ns equilibrium of peptide on the surfaces. In the pulling simulations, the water boxes are enlarged to 30 Å × 30 Å × 90 Å (Fig. 2(b)) involving about 11 212 to 11 298 atoms. The peptide is pulled along the direction perpendicular to the substrates. In order to simulate the process of peeling peptide from metal surfaces, a dummy atom was linked to one end of peptide with a constraint force constant $K = 8$ kcal/mol/Å^2. By fixing the metal surfaces and pulling the dummy atom in the designated direction under a constant pulling velocity, steered MD simulations were performed to simulate an AFM experiment [24,25]. Analyses of trajectories are performed using the molecular graphics software Visual Molecular Dynamics (VMD) [26].

Analysis of the trajectories is mainly concentrated on the equilibrium properties. The intermolecular interactions between the peptide and the metal surfaces are investigated via pair correlation function (PCF). And we also performed dynamic simulations to pull the peptide far away from the metal surfaces to test the binding strength directly. At the third part of the analysis of the results, we calculate the root mean square displacement (RMSD) of the peptide in the absence and presence of the metal surfaces, respectively, which provide intrinsic information to understand the behavior of peptide adsorption on the metal surfaces.

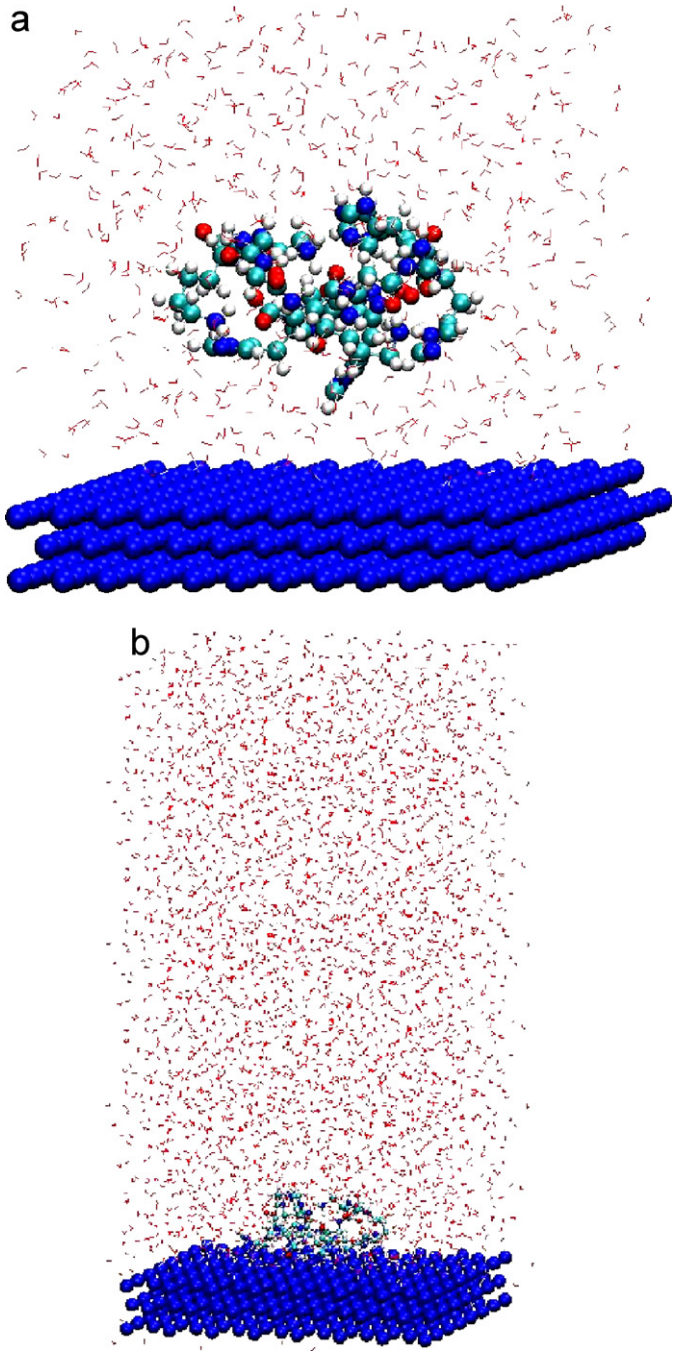

Fig. 2. Water boxes including the metal (1 0 0) surface and the His-tagged peptide.

3. Results and discussion

3.1. Adsorption energy

In the simulations, the His-tagged peptide interacts with three metal surfaces in water at 298 K. Meanwhile, MD simulations are implemented with the peptide in different

possible configurations on the metal surfaces and calculate the adsorption energy. So the configuration with the maximal adsorption energy is chosen as the initial simulation states. The peptide adsorbed on the metal surfaces after equilibrium is shown in Fig. 3. About half of imidazoles in the peptide can be observed to be parallel to the substrate, with a trend to maximize the contact area, which increase the adhesion energy and stabilizes the peptide on the metal substrate.

The adsorption energy of Lys, His, Gly on the metal surfaces is investigated, respectively. The adsorption energy of single amion acid on surfaces, which is listed in Table 2, confirmed that the amion acid of His is the primary contribution to the peptide–metal surfaces interaction. And the amino acids show the lowest adsorption energy on the Ni (1 0 0) surface, which is about 10–20 kcal/mol lower than that on the other two surfaces. In addition, the imidazole ring of His plays an important role in the adsorption, so the $6\times$ His-tag can consolidate the adsorption strength dramatically.

3.2. Static properties

PCF [27] is used to analyze the intermolecular interactions of the peptide in the absence and presence of metal surfaces. The PCF $G(r)$ can be expressed as [16]

$$G(r)=\frac{\langle\rho(r)\rangle}{\langle\rho_A\rangle_{local}}=\frac{1}{\langle\rho_A\rangle_{local}}\frac{1}{N_B}\sum_i\sum_j\frac{\delta(r_{ij}-r)}{V(r)}, \tag{2}$$

where $\rho(r)$ is the density of type A particles at distance r from particle B. The summation term shows the number of ij pairs that are separated by a distance r. These pairs are determined by taking spherical shells with volume $V(r)$ and normalized with the average density $\langle\rho\rangle_{local}$ in the whole volume and the total number of B particles (N_B). The PCF $G(r)$ is related to the probability of finding the center of a particle in a given distance from the center of another particle.

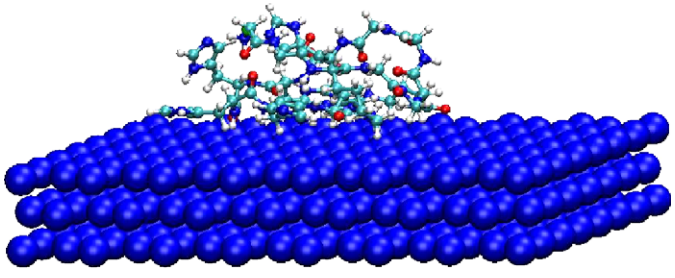

Fig. 3. The His-tagged peptide adsorption on the metal surface.

Table 2
Simulated adsorption energies of amino acids interaction with metal surfaces by MD

	Gly	His	Lys
Ni (1 0 0)	−54.41	−171.31	−141.48
Cu (1 0 0)	−48.28	−155.64	−124.84
Au (1 0 0)	−44.42	−145.77	−123.90

Energy values are given in kcal/mol.

When the peptide is equilibrated alone in the water box, the intermolecular interactions of the peptide chain with surrounding water molecules are shown in Fig. 4. The interactions between oxygen atoms of water molecules and hydrogens of His-tagged peptide versus the interactions between hydrogen atoms of water molecule and oxygen atoms of peptide are shown in Fig. 4(a). Strong H-bond between the oxygen of peptide and the hydrogen of water molecules can be observed at the distance of about 1.8 Å. The interactions between the non-hydrogen atoms of His-tagged peptide and water molecules are presented in Fig. 4(b). The peak at the distance of about 2.0 Å shows that the oxygen atoms of the peptide have stronger affinity to water molecules than the other atoms. Fig. 4(c) represents the PCF between water molecules and the three amino acid residues: Gly, Lys and His. The head group of Gly is a amidogen which can form H-bond easily in the water solvent, and this is demonstrated in PCF which shows Gly has better affinity to the water molecules than Lys and His.

The intermolecular interactions of the His-tagged peptide chains with the water molecules in the presence of metal surfaces are shown in Fig. 5. The polar atom N of the amino acid Gly interacts with the water molecules at a distance of about 2.5 Å, which is a weak hydrogen bond and is shown in Fig. 5(a). The binding affinity of the C^{α} atom of amino acid Lys is so weak at the interaction distance of about 4 Å, which can be observed in Fig. 5(b). The PCF between nitrogen atom (without hydrogen) and the water molecules in the absence of three different metal surfaces are given in Fig. 5(c), which shows that this nitrogen with a lone pair electron does not have strong affinity to the water molecules.

The intermolecular interactions of the His-tagged peptide chains with the metal surfaces are presented in Fig. 6. The side group of Gly is weak binder for all three metal surfaces, which can be observed in Fig. 5(a). The distances between the residue Gly and metal surfaces exceed 4 Å. The similar phenomena appear when Lys interacts with the metals surface. The distances between the residues and the surfaces are over 3.0 Å (Fig. 6(b)). The –OH group in strong binder lies relatively closer with the metal surface [16], which can also be observed in Fig. 5(c). It can be concluded that His is the stronger binder in this sequence for the Ni, Cu, Au (1 0 0) surfaces. This is also demonstrated by the behavior of the residues His in equilibrium process, the imidazole rings trending to be parallel to the substrate with the lowest adsorption energy on the metal surfaces.

3.3. Dynamics properties (binding strength)

In order to investigate the dynamic properties of the peptide near the metal surfaces, we perform MD simulation

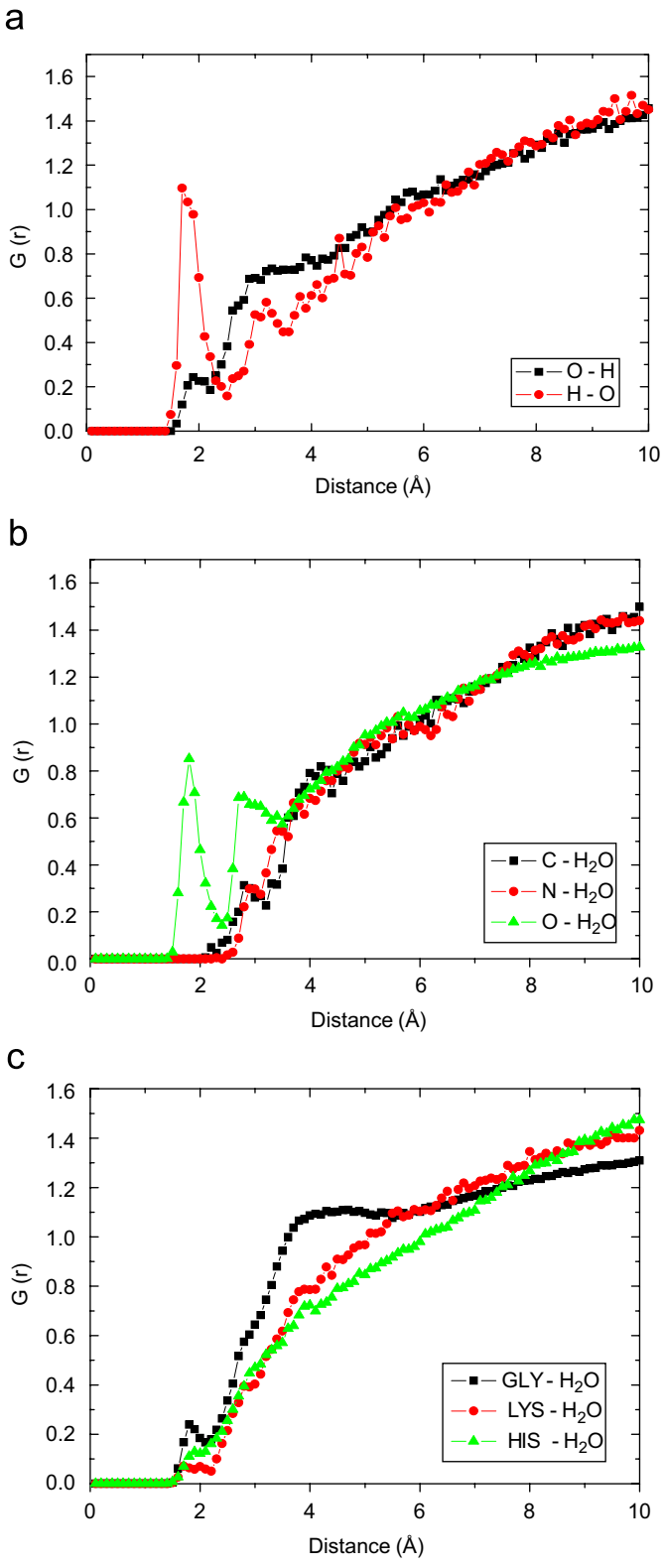

Fig. 4. PCF between water molecule and residues of His-tagged peptide (with no metal surfaces). (a) Oxygen of H_2O between the hydrogen of the peptide. (b) The heavy atoms (C, N, O) between oxygen of H_2O. (c) Amino acid residues between oxygen of H_2O.

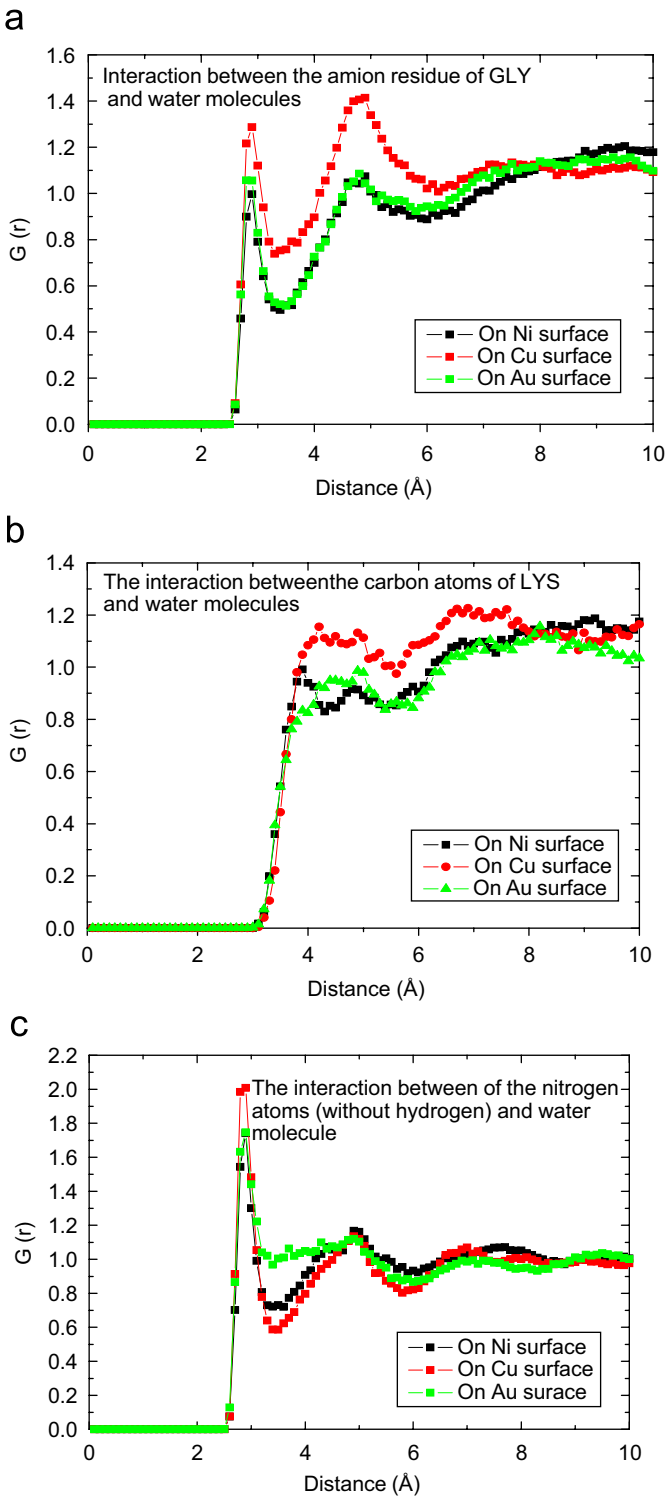

Fig. 5. PCF between residues of His-tagged peptide and water molecule in presence of metal surfaces: (a) Gly between oxygen of H_2O; (b) Lys between oxygen of H_2O; (c) His between oxygen of H_2O.

to pull the peptide from the metal surfaces after the adsorption equilibrium. Relaxation time is the key parameters of polymer solution dynamics, as it directly correlates with the different modes of molecule motion and hydrodynamic properties of the solution. Near the

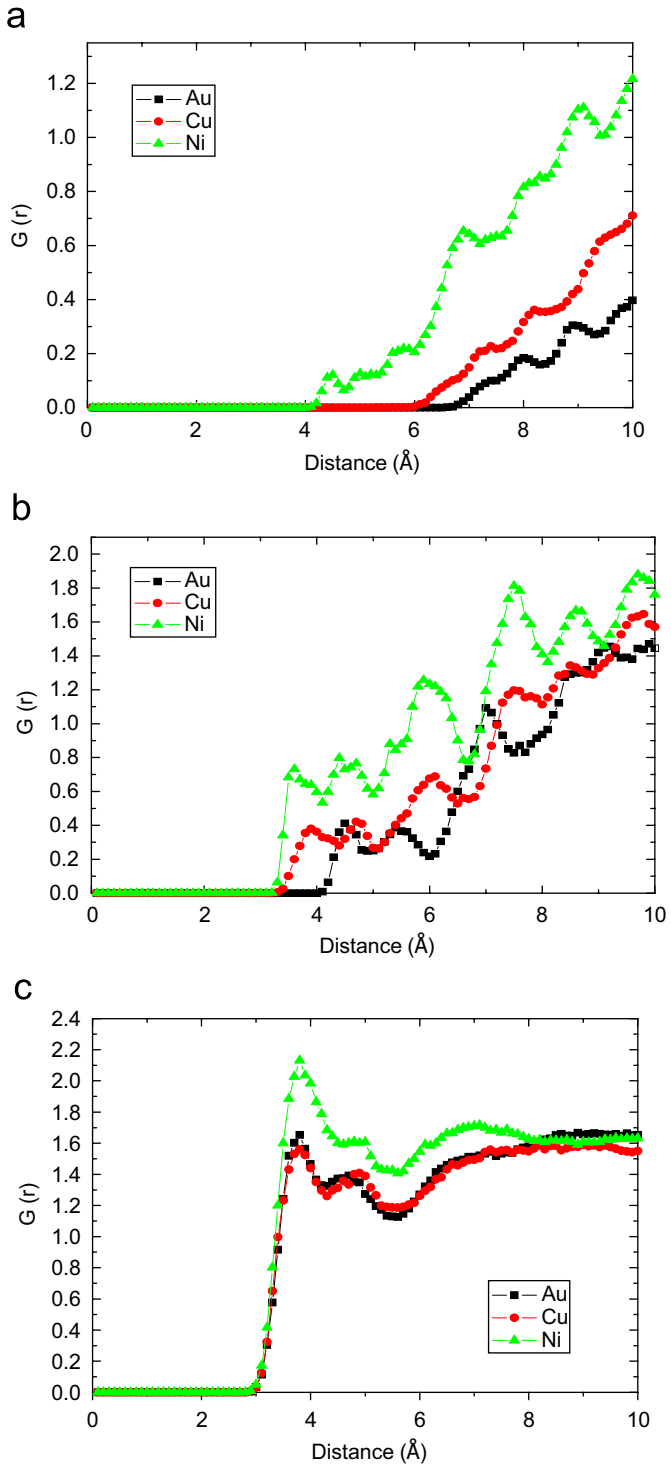

Fig. 6. PCF between metal surfaces and: (a) side group of Gly; (b) side group of Lys; (c) side group of His.

equilibrium, the motion of a macromolecule is best described by the longest relaxation time [28]. For the MD simulation of the dynamic properties, the time scales of protein stretching and peeling are estimated to predict the simulation time and the time scale of the peeling model is based on quasi-static condition [29]. Compared with adhesion energy and elasticity energy, both the work of solvent viscosity and kinetic energy should be neglected.

The total energy of adhesion and elasticity E_T, the work of solvent viscosity E_v and the kinetic energy E_k can be expressed, respectively, as [29]

$$E_T = \left(\frac{1}{2}k\varepsilon^2 + \Delta\gamma\right)L, \quad E_v = \eta_0 L^2 \frac{\mathrm{d}L}{\mathrm{d}t}, \quad E_k = \frac{1}{2}\rho L v^2, \tag{3}$$

where k is the stretch modulus of proteins, ε the strain, $\Delta\gamma$ the adhesion energy per unit length, η_0 the solvent dynamic viscosity coefficient, ρ the line density of proteins, L the pulling length, and v the pulling velocity. To neglect the work of solvent viscosity and kinetic energy means $E_T \gg E_v$ and $E_T \gg E_k$, so we can get two characteristic time $\tau_v = (2\eta_0 L^2/k\varepsilon^2 + 2\Delta\gamma)$ and $\tau_k = L\sqrt{(2\rho/k\varepsilon^2 + 2\Delta\gamma)}$. We estimate that $L \approx 1\,\mathrm{nm}$, $k \approx 10^3\,\mathrm{pN}$ [30], $\Delta\gamma \approx 10^2\,\mathrm{pN}$, $\rho \approx 10^{-10}\,\mathrm{kg/m}$ and $\eta_0 \approx 10^{-3}\,\mathrm{Pas}$ [31], assuming $\varepsilon \sim 0.1$, so the time scale in peeling of proteins is estimated as $\tau \gg \mathrm{Max}(\tau_v, \tau_k) \sim 10^{-11}\,\mathrm{s}$. In our simulation, the peeling process is performed in about 1.2 ns, which is much larger than τ. So the pulling process can be taken as a quasi-static process.

For the MD simulation of pulling process, we perform simulations of pulling the synthetic peptide in aqueous solvent at a constant velocity ($v = 0.04\,\mathrm{Å/ps}$). Similar peeling simulations have been performed to investigate ssDNA interacting with graphite surface [31] and structural stability of proteins in the solution and on the surface [29]. Both the pulling directions are perpendicular to the metal surfaces. We obtain the curves of pulling force vs. time for the dynamics process shown in Fig. 7. The biggest peak forces are about 7500, 6500 and 6000 pN for the His-tagged peptide being pulled from Ni, Cu and Au surfaces, respectively. These values are far more than the force to break a H-bond, which may be due to the fact that the peeling velocity is very fast and the viscosity of the water molecules induces the resistance force. We have simulated

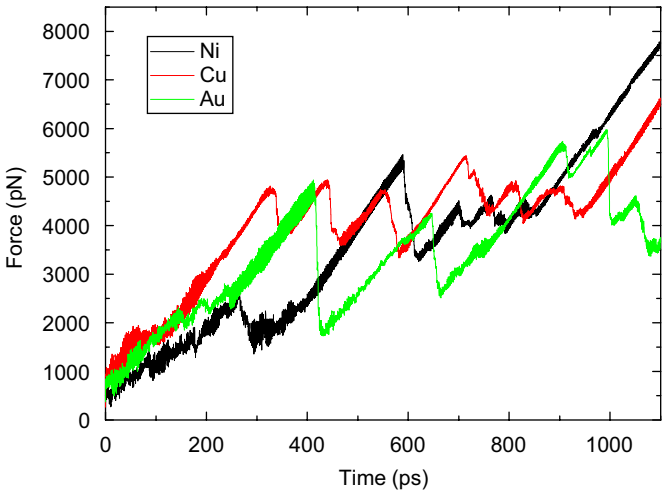

Fig. 7. Peel off force of the His-tagged peptide adhering to metal substrate in the water solvent.

the peeling processes in vacuum and found the forces decrease a lot. It can be attributed to the H-bonds between the peptide and water molecules. In the pulling process, the H-bonds build a net-like structure which resists the pulling in the reverse direction and increases the force to implement the pulling process. But we compare the pulling force with the same aqueous circumstances and parameters. So the water-mediated effects can be eliminated when we investigate the difference of binding strength.

3.4. Root-mean-square displacement/deviation (RMSD)

Fitting is the procedure whereby two or more conformations of the same or different molecules are oriented in space so that particular atoms or functional groups are optimally superimposed upon each other. The objective of the fitting procedure is to find the relative orientations of the molecules in which this function is minimized. The most common measure of the fit between two structures is the RMSD between pairs of atoms.

Mean-square displacement provides a means to follow the quantitative conformational changes upon binding. The expression of RMSD is given by [32]

$$\Delta d(t) = \left[\frac{1}{N}\sum_{1}^{N}(d_i(t) - d_i(0))^2\right]^{1/2}, \quad (4)$$

where N is the number of atoms over which the RMSD is measured, $d_i(t)$ and $d_i(0)$ are the coordinates of the atoms i at time t and at a reference time, respectively.

Analysis of RMSDs between coordinate sets of the backbone atoms of the starting structures and corresponding average structures calculated during MD simulations also demonstrate the adsorption of the peptide on metal surfaces. The average structures are calculated for the time intervals: 0–300–600–900–1200 ps. The corresponding RMSDs for the His-tagged peptide in the solvent are shown in Table 3. Fig. 8 shows the RMSDs of all-atom of the His-tagged peptide during the processes of adsorption to the metal surfaces. RMSDs of C^{α} atoms of backbone in the presence of metal surfaces are shown in Fig. 9. The values for the peptide adsorption on nickel surface are the smallest, which means the His-tagged peptide adsorption on nickel surface is the most stable. It is clearly shown that the conformational flexibility and possible rearrangements are dependent on the adsorption. In other words, the interactions between the peptide and the metal surfaces

Table 3
RMSD values between conformations of His-tagged peptide in a single MD run with no metal surface

Frames (ps)	RMSD (Å)
1–300	1.352
300–600	0.926
600–900	1.622
900–1200	2.649

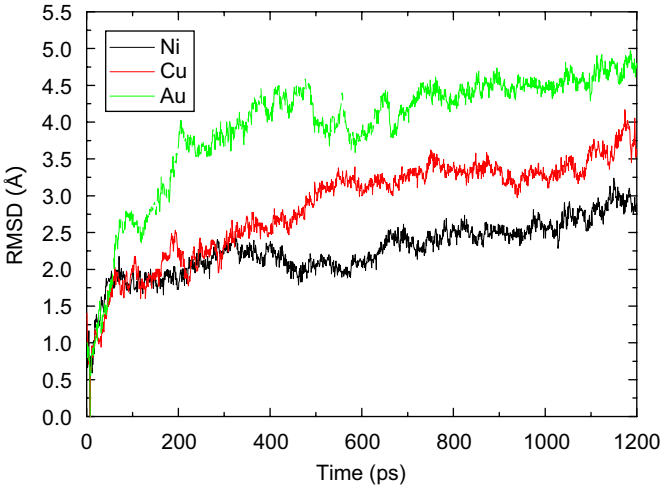

Fig. 8. RMSDs of His-tagged peptide with metal surfaces.

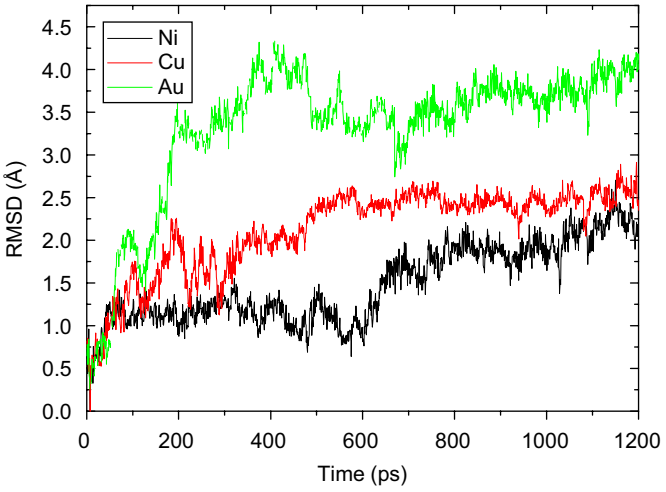

Fig. 9. RMSDs of C^{α} atoms of backbone in the presence of metal surface.

limit the vibration of His-tagged peptide. It can be understood from the viewpoint of thermodynamics. Conformational entropy plays the most important role in the process of adsorption [33]. The binding of a ligand to a protein or the adsorption of a peptide on a membrane involves an entropy loss [34]. The adsorption of this peptide on the metal surfaces also results in the loss of entropy, because the motion is limited by the interaction, including translational and rotational degrees of freedom.

4. Conclusion

Understanding the interaction between organic molecules and metal surfaces is of crucial importance in fundamental studies as well as in various applications such as catalysis coatings, lubrication, corrosion inhibition, molecular devices, and so on. MD simulations are performed to investigate the adsorption behavior of His-tagged peptide on three metal surfaces. We analyzed some equilibrium and dynamics properties of His-tagged peptide chain that should be important for selective surface

binding. And we also compare the characteristics of the three amino acids in the peptide sequence interacting with Ni, Cu, Au surfaces, which shows that His is the strongest binder among them.

The RMSD values demonstrate that in the presence of metal surfaces the conformational rearrangements are significantly constrained. It appears that the entropy loss due to the binding with reduced flexibility is an important aspect of binding, which thus should be compensated with the affinity of the binding residues for the binding stability.

Acknowledgments

This research was supported by Distinguished Young Scholar Fund of National Natural Science Foundation of China (NSFC, Grant no. 10225209), key project from Chinese Academy of Sciences (Grant no. KJCX-SW-L2).

References

[1] Moresco F, Meyer G, Rieder KH, Tang H, Gourdon A, Joachim C. Conformational changes of single molecules induced by scanning tunneling microscopy manipulation: a route to molecular switching. Phys Rev Lett 2001;86(4):672–5.
[2] Kühnle A, Linderoth TR, Hammer B, Besenbacher F. Chiral recognition in dimerization of adsorbed cysteine observed by scanning tunnelling microscopy. Nature 2002;415(6874):891–3.
[3] Sarikaya M, Tamerler C, Jen AKY, Schulten K, Baneyx F. Molecular biomimetics: nanotechnology through biology. Nat Mater 2003;2(9):577–85.
[4] Jeffrey JG. The interaction of proteins with solid surfaces. Curr Opin Struct Biol 2004;14:110–5.
[5] Seeman NC, Belcher AM. Emulating biology: building nanostructures from the bottom up. Proc Natl Acad Sci USA 2002;99(Suppl. 2):6451–5.
[6] Montemagno C, Bachand G. Constructing nanomechanical devices powered by biomolecular motors. Nanotechnology 1999;10(3):225–31.
[7] Calonder C, Tie Y, Van Tassel PR. History dependence of protein adsorption kinetics. Proc Natl Acad Sci USA 2001;98(19):10664–9.
[8] Malmsten M. Ellipsometry studies of fibronectin adsorption. Colloids Surf B-Biointerfaces 1995;3(6):371–81.
[9] Wertz CF, Santore MM. Adsorption and relaxation kinetics of albumin and fibrinogen on hydrophobic surfaces: single-species and competitive behavior. Langmuir 1999;15(26):8884–94.
[10] Schunack M, Rosei F, Naitoh Y, Jiang P, Gourdon A, Laegsgaard E, Stensgaard I, Joachim C, Besenbacher F. Adsorption behavior of Lander molecules on Cu(1 1 0) studied by scanning tunneling microscopy. J Chem Phys 2002;117(13):6259–65.
[11] Delle Site L, Abrams CF, Alavi A, Kremer K. Polymers near metal surfaces: selective adsorption and global conformations. Phys Rev Lett 2002;89(15):156103.
[12] Delle Site L, Alavi A, Abrams CF. Adsorption energies and geometries of phenol on the (1 1 1) surface of nickel: an ab initio study. Phys Rev B 2003;67(19):193406.
[13] Mittendorfer F, Hafner J. A DFT study of the adsorption of thiophene on Ni(1 0 0). Surf Sci 2001;492(1–2):27–33.
[14] Mittendorfer F, Hafner J. Density-functional study of the adsorption of benzene on the (1 1 1) (1 0 0) and (1 1 0) surfaces of nickel. Surf Sci 2001;472(1–2):133–53.
[15] Braun R, Sarikaya M, Schulten K. Genetically engineered gold-binding polypeptides: structure prediction and molecular dynamics. J Biomater Sci Polym Ed 2002;13(7):747–57.
[16] Kantarci N, Tamerler C, Sarikaya M, Haliloglu T, Doruker P. Molecular dynamics simulations on constraint metal binding peptides. Polymer 2005;46(12):4307–13.
[17] William LJ, Jayaraman C, Jeffry DM, Roger WI, Michael LK. Comparison of simple potential functions for simulating liquid water. J Chem Phys 1983;79(2):926–35.
[18] Kohlmeyer A, Spohr W, Witschel E. Molecular dynamics simulations of water/metal and water/vacuum interfaces with a polarizable water model. Chem Phys 1996;213(1–3):211–6.
[19] Brooks BR, Bruccoleri RE, Olafson BD, States DJ, Swaminathan S, Karplus M. CHARMM: a program for macromolecular energy, minimization, and dynamics calculations. J Comput Chem 1983;4(2): 187–217.
[20] Mackerell AD, Wiorkiewiczkuczera J, Karplus M. An all-atom empirical energy function for the simulation of nucleic-acids. J Am Chem Soc 1995;117(48):11946–75.
[21] Stauffer D. Annual reviews of computational physics IX. Germany: Cologne University; 2001.
[22] Berendsen HJC, Postma JPM, Van Gunsteren WF, DiNola A, Haak JR. Molecular dynamics with coupling to an external bath. J Chem Phys 1984;81(8):3684–90.
[23] Ryckaert JP, Ciccotti G, Berendsen HJC. Numerical integration of the cartesian equations of motion of a system with constraints: molecular dynamics of *n*-alkanes. J Comput Phys 1977;23(3): 327–41.
[24] Grubmüller H, Heymann B, Tavan P. Ligand binding: molecular mechanics calculation of the streptavidin-biotin rupture force. Science 1996;271(5251):997–9.
[25] Merkel R, Nassoy P, Leung A, Ritchire K, Evans E. Energy landscapes of receptor-ligand bonds explored with dynamic force spectroscopy. Nature 1999;397(6714):50–3.
[26] Humphrey W, Dalke A, Schulten K. VMD: visual molecular dynamics. J Mol Graphics 1996;14(1):33–8.
[27] Stillinger FH, Rahman A. Improved simulation of liquid water by molecular dynamics. J Chem Phys 1974;60(4):1545–57.
[28] Wong PK, Lee YK, Ho CM. Deformation of DNA molecules by hydrodynamics focusing. J Fluid Mech 2003;497:55–65.
[29] Yin J, Zhao YP, Zhu RZ. Molecular dynamics simulation of barnacle cement. Mater Sci Eng A 2005;409(1–2):160–6.
[30] Smith SB, Cui YJ, Bustamante C. Overstretching B-DNA: the elastic response of individual double-stranded and single-stranded DNA molecules. Science 1996;271(5250):795–9.
[31] Shi XH, Kong Y, Zhao YP, Gao HJ. Molecular dynamics simulation of peeling a DNA molecule on substrate. Acta Mech Sin 2005;21(3):249–56.
[32] Leach AR. Molecular modeling principles and applications. 2nd ed. London: Prentice-Hall; 2001.
[33] Delle Site L, Leon S, Kremer K. BPA-PC on a Ni(1 1 1) surface: the interplay between adsorption energy and conformational entropy for different chain-end modifications. J Am Chem Soc 2004;126(9): 2944–55.
[34] Ben-Tal N, Honig B, Bagdassarian CK, Ben-Shaul A. Association entropy in adsorption processes. Biophys J 2000;79(3):1180–7.